A Simultaneous Augmented Lagrange Approach for the Simulation of Soft Biological Tissue

AQ1

Dirk Böse[1], Sarah Brinkhues[2], Raimund Erbel[1], Axel Klawonn[3], Oliver Rheinbach[3], and Jörg Schröder[2]

[1] Westdeutsches Herzzentrum, Universitätsklinikum Essen
[2] Fakultät für Ingenieurwissenschaften, Abteilung Bauwissenschaften, Institut für Mechanik, Universität Duisburg-Essen
[3] Lehrstuhl für Numerische Mathematik und Numerische Simulation, Fakultät für Mathematik, Universität Duisburg-Essen. Germany.
`{axel.klawonn, oliver.rheinbach}@uni-duisburg-essen.de`

Summary. In this paper, we consider the elastic deformation of arterial walls as occurring, e.g., in the process of a balloon angioplasty, a common treatment in the case of atherosclerosis. Soft biological tissue is an almost incompressible material. To account for this property in finite element simulations commonly used free energy functions contain terms penalizing volumetric changes. The incorporation of such penalty terms can, unfortunately, spoil the convergence of the nonlinear iteration scheme, i.e., of Newton's method, as well as of iterative solvers applied for the solution of the linearized systems of equations. We show that the augmented Lagrange method can improve the convergence of the linear and nonlinear iteration schemes while, at the same time, implementing a guaranteed bound for the volumetric change. Our finite element model of an atherosclerotic arterial segment, see Fig. 1, is constructed from intravascular ultrasound images; for details see [4].

this figure will be printed in b/w

Fig. 1. Finite element model of an atherosclerotic arterial segment 1.3M unknowns

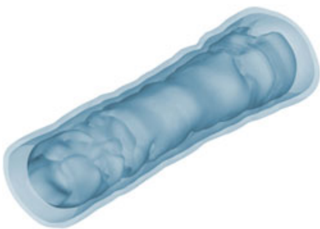

R. Bank et al. (eds.), *Domain Decomposition Methods in Science and Engineering XX*, Lecture Notes in Computational Science and Engineering 91,
DOI 10.1007/978-3-642-35275-1_43, © Springer-Verlag Berlin Heidelberg 2013

1 Nonlinear Model and Algorithm

Biological tissues, such as arteries, are fiber enforced materials composed of an almost incompressible matrix substance with embedded collagen fibers. The arrangement of the fibers in arterial walls is characterized by two preferred directions helically wound along the artery. The material behavior of the collagen fiber bundles is represented by the superposition of two transversely isotropic models; see [12]. Thus, the strain energies are given by

$$\psi = \psi^{\mathrm{iso}}(\mathbf{C}) + \psi^{\mathrm{ti},(1)}(\mathbf{C},\mathbf{M}^{(1)}) + \psi^{\mathrm{ti},(2)}(\mathbf{C},\mathbf{M}^{(2)})\,. \tag{1}$$

Here, $\mathbf{F} := \nabla\varphi$ is the deformation gradient, $\mathbf{C} := \mathbf{F}^T\mathbf{F}$ the right Cauchy-Green-tensor, and $\mathbf{M}^{(a)} := \mathbf{a}^{(a)} \otimes \mathbf{a}^{(a)}$, $a = 1,2$ are the structural tensors characterizing the fiber directions. There exist different possibilities to model the mechanical response of soft biological tissue; see, e.g., [2, 12]. We are interested in polyconvex energy functions. For the construction of anisotropic, polyconvex functions, see, e.g., [18]. Here, we use the model due to [12], which was denoted model ψ_B in [3],

$$\psi = c_1\left(I_1 I_3^{-1/3} - 3\right) + \sum_{a=1}^{2} \frac{k_1}{2k_2}\left\{\exp\left(k_2\left\langle J_4^{(a)} I_3^{-1/3} - 1\right\rangle^2\right) - 1\right\}$$
$$+\, \varepsilon_1\left(I_3^{\varepsilon_2} + I_3^{-\varepsilon_2} - 2\right)^{\alpha},$$

with the invariants $I_1 = \mathrm{tr}\,\mathbf{C}, I_2 = \mathrm{tr}[\mathrm{Cof}(\mathbf{C})], I_3 = \det\mathbf{C}, J_4^{(a)} = \mathrm{tr}[\mathbf{C}\mathbf{M}^{(a)}]$, $J_5^{(a)} = \mathrm{tr}[\mathbf{C}^2\mathbf{M}^{(a)}]$. Here, $\langle\bullet\rangle$ denote the Macauly brackets, $\langle\bullet\rangle = (|\bullet| + \bullet)/2$. The penalty term $\varepsilon_1\left(I_3^{\varepsilon_2} + I_3^{-\varepsilon_2} - 2\right)^{\alpha}$ models the incompressibility.

We adjust our parameters to experimental results in [11]; for details, see [5]. The adjustment results in the parameters $c_1 = 7.17\,[\mathrm{kPa}], k_1 = 3.69e-3\,[\mathrm{kPa}], k_2 = 51.2$ for the adventitia and $c_1 = 9.23\,[\mathrm{kPa}], k_1 = 193\,[\mathrm{kPa}], k_2 = 2.627e3$ for the media.

In the augmented Lagrange approach [10, 20] a Lagrange multiplier is introduced on each finite element and $\mu^T(\det\mathbf{F} - \mathbf{1})$ is added to the energy ψ. Here, we mean by $\det\mathbf{F}$ the vector of element-wise determinants of $\mathbf{F}$. The Lagrange multiplier will be computed iteratively by an Uzawa-like iteration $\mu_{k+1} = \mu_k + \xi_k(\det\mathbf{F} - \mathbf{1})$, where in our computations in Sect. 3 the series ξ_k will be chosen as a constant $\xi_k = \xi = 499.0$. We have chosen ξ by hand from the set $\{99, 499, 999, 1999, 9999\}$.

Our parameter fit is performed assuming incompressibility of the material. When using the penalty approach we have to choose sufficiently large penalty parameters. Here, our penalty parameters are $\varepsilon_1 = 70.0\,[\mathrm{kPa}], \varepsilon_2 = 8.5, \alpha = 1$ for the adventitia and $\varepsilon_1 = 360.0\,[\mathrm{kPa}], \varepsilon_2 = 9.0, \alpha = 1$ for the media. Also in the augmented Lagrange approach we need to choose our penalty parameters but here the penalty may be relaxed significantly, i.e., we choose $\varepsilon_1 = 10.0\,[\mathrm{kPa}], \varepsilon_2 = 4.0, \alpha = 1$ for adventitia and media. The relaxation becomes evident when the penalty function is plotted for the different sets of parameters. A sufficiently accurate stopping criterion has to be chosen for the augmented Lagrange loop; here we chose a tolerance of $|\det(\mathbf{F}) - 1| \leq 0.01$ on each element.

In our discretization, we have to avoid locking effects. We therefore replace point-wise penalization by the penalization of the average volumetric change on every finite element. This is accomplished, as in [3, 16], by applying a three-field formulation, known as the $\bar{\mathbf{F}}$-approach; see [19]. We use 10-noded tetrahedral elements for the displacement.

In our nonlinear scheme we solve a sequence of linear problems obtained from Newton's method, see, e.g., Fig. 2. This is also referred to as (pseudo) time stepping or load stepping. To obtain a fair comparison, we have chosen an automatic time stepping strategy. For the penalty approach we increase Δt when the number of Newton iterations is smaller than 6 and decrease Δt when it is larger than 9. This choice produced the best results. The simultaneous Augmented Lagrange approach, where the iteration for the Lagrange multiplier simultaneously to the Newton correction, can be viewed as an inexact Newton method. Thus, a quadratic convergence cannot be expected. We therefore have chosen the bounds for the auto time stepping as 18 and 36. For all approaches the maximal time step size was bounded by $\Delta t_{\max} = 0.4$.

Fig. 2. Penalty for the incompressibility

Nonlinear Iteration (Penalty)

Set $k = 0$ and $t_0 = \Delta t_0$;
Apply partial load $t_k \cdot \mathbf{f}_{\text{load}}$ if the full load is not yet reached;
  Use Newton iteration to solve the nonlinear problem.
    Use GMRES to solve linearized problem using the
    FETI domain decomposition method as a preconditioner;
    Apply Newton correction;
  Adapt load step size Δt_{k+1}, i.e.,
  $\Delta t_{k+1} = 10^{1/5} \Delta t_k$, $\Delta t_{k+1} = 10^{-1/5} \Delta t_k$, or $\Delta t_{k+1} = \Delta t_k$;
  Set $t_{k+1} = t_k + \Delta t_{k+1}$;

2 FETI-DP Method

We briefly introduce the well-known FETI-DP method. For a more detailed introduction, see, e.g., [13, 16, 17, 21]. For algorithms of the **F**inite **E**lement **T**earing and **I**nterconnecting-type (FETI); see [6–9]. Using FETI-DP methods linear systems with billions of unknowns have been solved, e.g., in [14, 16] on large parallel machines (Fig. 3).

AQ2 AQ3

We decompose the domain Ω into N nonoverlapping subdomains Ω_i. For all subdomains Ω_i, we assemble the local stiffness matrices $\mathbf{K}^{(i)}$ and local load vectors $\mathbf{f}^{(i)}$, $i = 1, \ldots, N$,

Fig. 3. Simultaneous augmented Lagrange for the incompressibility [10, 20]

Nonlinear Iteration (Simultaneous Augmented Lagrange)

Set $k=0$ and $t_0=\Delta t_0$;
Apply partial load $t_k \cdot \mathbf{f}_{\text{load}}$ if the full load is not yet reached;
  Set Lagrange parameter $\mu_0=0$;
  While Newton iteration has not converged and while elements with $|\det(\mathbf{F}) - 1| \geq$ TOL exist: Solve nonlinear problem with simultaneous Newton iteration and iteration for μ
    Use GMRES to solve linearized problem using the FETI method
    Apply Newton correction and update Lagrange parameter $\mu_{k+1}=\mu_k+\xi_k(\det\mathbf{F}-1)$;
  Adapt load step size Δt_{k+1}, i.e., $\Delta t_{k+1}=10^{1/5}\Delta t_k$, $\Delta t_{k+1}=10^{-1/5}\Delta t_k$, or $\Delta t_{k+1}=\Delta t_k$.
  Set $t_{k+1}=t_k+\Delta t_{k+1}$;

$$\mathbf{K}=\begin{bmatrix}\mathbf{K}^{(1)} & & \\ & \ddots & \\ & & \mathbf{K}^{(N)}\end{bmatrix}, \mathbf{u}=\begin{bmatrix}\mathbf{u}^{(1)}\\ \vdots \\ \mathbf{u}^{(N)}\end{bmatrix}, \mathbf{f}=\begin{bmatrix}\mathbf{f}^{(1)}\\ \vdots \\ \mathbf{f}^{(N)}\end{bmatrix}.$$

The interface is $\Gamma=\cup_{i=1}^{N}\partial\Omega_i \setminus \partial\Omega$. The discrete problem can be formulated as minimization problem with the interface continuity constraint $\mathbf{Bu}=\mathbf{0}$, where $\mathbf{B}=[\mathbf{B}^{(1)},\ldots,\mathbf{B}^{(N)}]$ with entries from $0,1,-1$. By introducing Lagrange multipliers λ to enforce the continuity along the subdomain interface we obtain the problem: Find $(\mathbf{u},\lambda)$, such that

$$\begin{aligned}\mathbf{Ku}+\mathbf{B}^T\lambda &= \mathbf{f}\\ \mathbf{Bu} \qquad &= \mathbf{0}.\end{aligned}$$

This problem can be solved by eliminating the displacement variables $\mathbf{u}$ and solving the resulting Schur complement system by conjugate gradients.

In FETI-DP methods some continuity constraints are enforced on *primal* displacement variables $\tilde{\mathbf{u}}_\Pi$ throughout iterations to enforce invertibility of the local problems. This yields a saddle point problem of the form

$$\begin{aligned}\widetilde{\mathbf{K}}\tilde{\mathbf{u}}+\mathbf{B}^T\lambda &= \tilde{\mathbf{f}}\\ \mathbf{B}\tilde{\mathbf{u}} \qquad &= \mathbf{0},\end{aligned}$$

where the matrix $\widetilde{\mathbf{K}}$ and right hand side $\tilde{\mathbf{f}}$ are partially assembled in the primal variables, i.e.,

$$\widetilde{\mathbf{K}} = \begin{bmatrix} \mathbf{K}_{BB}^{(1)} & & & \widetilde{\mathbf{K}}_{\Pi B}^{(1)T} \\ & \ddots & & \vdots \\ & & \mathbf{K}_{BB}^{(N)} & \widetilde{\mathbf{K}}_{\Pi B}^{(N)T} \\ \widetilde{\mathbf{K}}_{\Pi B}^{(1)} & \cdots & \widetilde{\mathbf{K}}_{\Pi B}^{(N)} & \widetilde{\mathbf{K}}_{\Pi\Pi} \end{bmatrix}, \qquad \tilde{\mathbf{f}} = \begin{bmatrix} \mathbf{f}_B^{(1)} \\ \vdots \\ \mathbf{f}_B^{(N)} \\ \tilde{\mathbf{f}}_{\Pi} \end{bmatrix}.$$

The coupling also provides the coarse problem for the method. Reducing the system of equations to an equation in λ, it remains to solve iteratively

$$\mathbf{M}_{\mathrm{D}}^{-1}\mathbf{F}_{feti}\lambda = \mathbf{M}_{\mathrm{D}}^{-1}\mathbf{d},$$

where $\mathbf{F}_{feti} = \mathbf{B}\widetilde{\mathbf{K}}^{-1}\mathbf{B}^T$, and $\mathbf{M}_{\mathrm{D}}^{-1} = \mathbf{B}_D\mathbf{R}_\Gamma^T\mathbf{S}\mathbf{R}_\Gamma\mathbf{B}_D^T$ is the Dirichlet preconditioner. Here, $\mathbf{S}$ is the Schur complement obtained by eliminating the interior variables in every subdomain, i.e., $\mathbf{S} = \begin{bmatrix} \mathbf{S}^{(1)} & & \\ & \ddots & \\ & & \mathbf{S}^{(N)} \end{bmatrix}$. The operator $\mathbf{R}_\Gamma$ is a restriction matrix, consisting of zeros and ones, that, when applied to a vector $\tilde{\mathbf{u}}$, removes the interior variables from $\tilde{\mathbf{u}}$. The matrices $\mathbf{B}_D$ are scaled variants of the jump operator $\mathbf{B}$ where, in the simplest case, the contribution from and to each interface node is scaled by the inverse of the multiplicity of the node. We define the multiplicity of a node as the number of subdomains it belongs to. For heterogeneous problems a more elaborate scaling, using an appropriate scaling factor, defined by the coefficients ρ_i, is necessary; see, e.g., [17, p. 1532, Formula (4.3)] and [15, p. 1403, Formula (6)].

3 Numerical Results

A pressure of 200 mmHg is applied to the inside of the artery, see Fig. 1. The FETI-DP iteration is stopped when the absolute residual is reduced to 5×10^{-9}; we have 224 subdomains. The total cost can be estimated by multiplying the number of Newton steps by the corresponding average number of (inner) FETI-DP Krylov iterations, see Tables 1 and 2.

Our results show that the use of the augmented Lagrange method can significantly improve the properties of the linearized systems occurring in the nonlinear solution scheme. The convergence of the nonlinear scheme is also improved, i.e., in our nonlinear scheme larger pseudo time steps Δt can be chosen. Of course, an additional iteration process for the Lagrange multiplier is introduced. Here, this iteration process is carried out simultaneously with the Newton iteration.

The results in Tables 1 and 2 show that the additional cost for the augmented Lagrange iteration is more than amortized by the faster convergence of the nonlinear scheme and the linear iterative solver. Moreover, in the augmented Lagrange approach the volumetric change is exactly controlled during the iteration process, i.e., we have satisfied element-wise the condition $|\det(\mathbf{F}) - 1| \leq 0.01$. In the penalty approach the volumetric change produced by the chosen penalty parameters is only

Table 1. Newton iteration for the penalty formulation. Pseudo-time t, number of Newton steps, average number of Krylov iterations per Newton step.

t	Newton steps	∅ Krylov its
0.010	9	172.2
0.020	5	173.0
0.036	5	175.8
0.061	5	179.4
0.101	6	189.3
0.141	5	187.0
0.204	6	201.8
0.267	5	195.6
0.367	7	208.0
0.467	7	204.1
0.567	5	207.4
0.725	6	217.8
0.884	5	225.4
1.135	6	242.0
1.386	6	253.8
1.637	7	266.3
1.889	5	279.4
2.000	4	285.8
	Σ 104	Total ∅ 213.3

Table 2. Simultaneous Newton and augmented Lagrange (AL) iteration. Pseudo-time t, number of Newton-AL steps, average number of Krylov iterations per Newton-AL step.

t	Newton-AL steps	∅ Krylov its
0.010	9	99.3
0.026	4	100.5
0.051	5	101.4
0.091	6	101.3
0.154	6	102.8
0.254	7	104.3
0.412	11	105.4
0.664	14	109.4
1.062	14	119.0
1.462	16	139.7
1.862	17	167.0
2.000	15	180.8
	Σ 124	Total ∅ 138.6

known ex-post. In our example the solution using the penalty approach only satisfies $|\det(\mathbf{F}) - 1| \leq 0.021$.

In the results in Table 2, we see that the number of Newton-AL-iterations increases during the simulation. This is due to the fact that in the beginning of the simulation only a very small number of finite elements violate the element-wise condition $|\det(\mathbf{F}) - 1| \leq 0.01$.

The results in, both, Tables 1 and 2 also show an increase of the FETI-DP iterations during the simulation. We believe that this may in part be due to an increasing influence of the incompressibility constraint during the simulation but also result from the exponential stiffening behavior of the fibers. In [1], we have observed that the anisotropies introduced to the material wall models by the terms modeling the fibers can have a visible impact on the convergence of the nonlinear iteration scheme as well as the convergence of the iterative linear solver. Ideas described in [16] may improve the convergence of domain decomposition solvers for such anisotropic problems.

Bibliography

[1] Daniel Balzani, Dominik Brands, Axel Klawonn, Oliver Rheinbach, and Jörg Schröder. On the mechanical modeling of anisotropic biological soft tissue and iterative parallel solution strategies. *Arch. Appl. Mech.*, 80(5):479–488, 2010.

[2] Daniel Balzani, Patrizio Neff, Jörg Schröder, and Gerhard A. Holzapfel. A polyconvex framework for soft biological tissues. Adjustment to experimental data. *Int. J. Solids Struct.*, 43(20):6052–6070, 2006.

[3] Dominik Brands, Axel Klawonn, Oliver Rheinbach, and Jörg Schröder. Modelling and convergence in arterial wall simulations using a parallel FETI solution strategy. *Comput. Methods Biomec.*, 11:569–583, 2008.

[4] Dominik Brands, Jörg Schröder, Axel Klawonn, Oliver Rheinbach, Dirk Böse, and Raimund Erbel. Numerical simulations of arterial walls based on ivus-data. *PAMM*, 9(1):75–78, 2009.

[5] Sarah Brinkhues, Axel Klawonn, Oliver Rheinbach, and Jörg Schröder. Parallel simulation of arterial walls. 2011. In preparation.

[6] Charbel Farhat, Michel Lesoinne, Patrick LeTallec, Kendall Pierson, and Daniel Rixen. FETI-DP: A dual-primal unified FETI method - part i: A faster alternative to the two-level FETI method. *Internat. J. Numer. Methods Engrg.*, 50:1523–1544, 2001.

[7] Charbel Farhat, Michel Lesoinne, and Kendall Pierson. A scalable dual-primal domain decomposition method. *Numer. Lin. Alg. Appl.*, 7:687–714, 2000.

[8] Charbel Farhat, Jan Mandel, and Francois-Xavier Roux. Optimal convergence properties of the FETI domain decomposition method. *Comput. Methods Appl. Mech. Engrg.*, 115:367–388, 1994.

[9] Charbel Farhat and Francois-Xavier Roux. A method of Finite Element Tearing and Interconnecting and its parallel solution algorithm. *Int. J. Numer. Meth. Engrg.*, 32:1205–1227, 1991.

[10] M. Fortin and A. Fortin. A generalization of Uzawa's algorithm for the solution of the Navier-Stokes equations. *Comm. Appl. Numer. Methods*, 1(5):205–208, 1985.

[11] Gerhard A. Holzapfel. Determination of material models for arterial walls from uniaxial extension tests and histological structure. *J. Theor. Biol.*, 238(2):290–302, 2006.

[12] Gerhard A. Holzapfel, Thomas C. Gasser, and Ray W. Ogden. A new constitutive framework for arterial wall mechanics and a comparative study of material models. *J. Elasticity*, 61(1–3):1–48, 2000.

[13] Axel Klawonn and Oliver Rheinbach. A parallel implementation of Dual-Primal FETI methods for three dimensional linear elasticity using a transformation of basis. *SIAM J. Sci. Comput.*, 28:1886–1906, 2006.

[14] Axel Klawonn and Oliver Rheinbach. Inexact FETI-DP methods. *Inter. J. Numer. Methods Engrg.*, 69:284–307, 2007.

[15] Axel Klawonn and Oliver Rheinbach. Robust FETI-DP methods for heterogeneous three dimensional linear elasticity problems. *Comput. Methods Appl. Mech. Engrg.*, 196:1400–1414, 2007.

[16] Axel Klawonn and Oliver Rheinbach. Highly scalable parallel domain decomposition methods with an application to biomechanics. *ZAMM - Z. Angew. Math. Mech.*, 90(1):5–32, July 2010.

[17] Axel Klawonn and Olof B. Widlund. Dual-Primal FETI Methods for Linear Elasticity. *Comm. Pure Appl. Math.*, 59:1523–1572, 2006.

[18] Jörg Schröder and Patrizio Neff. Invariant formulation of hyperelastic transverse isotropy based on polyconvex free energy functions. *Int. J. Solids Struct.*, 40:401–445, 2003.

[19] Juan C. Simo. Numerical analysis and simulation of plasticity. In P.G. Ciarlet and J.L. Lions, editors, *Handbook of numerical analysis*, volume IV. Elsevier, 1998.

[20] Juan C. Simo and Robert L. Taylor. Quasi-incompressible finite elasticity in principal stretches. continuum basis and numerical algorithms. *Comput. Methods Appl. Mech. Engrg.*, 85(3):273–310, 1991.

[21] Andrea Toselli and Olof B. Widlund. *Domain Decomposition Methods - Algorithms and Theory*, volume 34 of *Springer Series in Computational Mathematics*. Springer-Verlag, Berlin Heidelberg New York, 2005.